Comparison and Uncertainty of Aerosol Optical Depth Estimates Derived from Spectral and Broadband Measurements

THOMAS CARLUND, TOMAS LANDELIUS, AND WEINE JOSEFSSON

Swedish Meteorological and Hydrological Institute, Norrköping, Sweden

(Manuscript received 2 September 2002, in final form 23 May 2003)

ABSTRACT

An experimental comparison of spectral aerosol optical depth $\tau_{a,\lambda}$ derived from measurements by two spectral radiometers [a LI-COR, Inc., LI-1800 spectroradiometer and a Centre Suisse d'Electronique et de Microtechnique (CSEM) SPM2000 sun photometer] and a broadband field pyrheliometer has been made. The study was limited to three wavelengths (368, 500, and 778 nm), using operational calibration and optical depth calculation procedures. For measurements taken on 32 days spread over 1 yr, the rms difference in $\tau_{a,\lambda}$ derived from the two spectral radiometers was less than 0.01 at 500 and 778 nm. For wavelengths shorter than 500 nm and longer than 950 nm, the performance of the LI-1800 in its current configuration did not permit accurate determinations of $\tau_{a,\lambda}$. Estimates of spectral aerosol optical depth from broadband pyrheliometer measurements using two models of the Ångström turbidity coefficient were examined. For the broadband method that was closest to the sun photometer results, the mean (rms) differences in $\tau_{a,\lambda}$ were 0.014 (0.028), 0.014 (0.019), and 0.013 (0.014) at 368, 500, and 778 nm. The mean differences are just above the average uncertainties of the sun photometer $\tau_{a,\lambda}$ values (0.012, 0.011, and 0.011) for the same wavelengths, as determined through a detailed uncertainty analysis. The amount of atmospheric water vapor is a necessary input to the broadband methods. If upper-air sounding data are not available, water vapor from a meteorological forecast model yields significantly better turbidity results than does using estimates from surface measurements of air temperature and relative humidity.

1. Introduction

As the design of instruments for spectral measurements of solar radiation evolves, and as the interest in and the request for spectral aerosol optical depth ($\tau_{a,\lambda}$) data increases, more and more stations with more and more sophisticated spectral radiometers are established almost all over the world. Even today, however, continuous spectral measurements are much sparser than broadband pyrheliometer measurements. Therefore, it is of great interest to utilize the available pyrheliometer measurements to derive the atmospheric turbidity and, further, to estimate $\tau_{a,\lambda}$. In Sweden, continuous pyrheliometer measurements have been made since 1983 at 12 sites and continuous spectral measurements for $\tau_{a,\lambda}$ determination are only made at two sites. One of these sites is at the Swedish Meteorological and Hydrological Institute (SMHI) in Norrköping, Sweden, from which data in this study are taken. The other site is a station within the Aerosol Robotic Network (AERONET; Holben et al. 1998), on the island of Gotland in the Baltic Sea. The question is how good $\tau_{a,\lambda}$ estimates from broadband measurements really are.

Corresponding author address: Thomas Carlund, SMHI, 601 76 Norrköping, Sweden.
E-mail: thomas.carlund@smhi.se

The original aim was to compare $\tau_{a,\lambda}$ estimates and observations at nine wavelengths in the 368–1024-nm range, using operational calibration and optical depth calculation procedures. Observations were to be made with two different spectral instruments, a three-channel sun photometer and simple spectroradiometer (300–1100 nm) and a broadband pyrheliometer. However, it turned out that the performance and calibration accuracy of the spectroradiometer were not good enough to be used as a reference. Therefore, the comparison is restricted to the three wavelengths (368, 500, 778 nm) of the sun photometer.

2. Measurements and methods

From March of 1999 to March of 2000, manual direct sun measurements with the spectroradiometer were taken when possible. The measuring site was the radiation measurement platform on the roof of SMHI (58.58°N, 16.15°E, 43 m altitude). Altogether, about 300 spectral scans from 32 different days during all seasons were recorded. At the research radiation station of SMHI, 1-min (mean values) radiation data are collected continuously. From this database, data from the sun photometer and the pyrheliometer at the times of the spectroradiometer scans were extracted.

a. Instruments

The spectroradiometer used was the manually operated LI-COR, Inc., LI-1800 portable spectroradiometer No. 178 [300–1100 nm, single monochromator, 6–7-nm bandwidth full width half maximum (FWHM), silicon photodetector, not temperature stabilized]. To scan the full wavelength range at 1-nm intervals took about 45 s. The instrument was equipped with a collimator to allow measurements of the direct solar radiation with a field of view (FOV) of 2.5° (full angle). The instrument was either operated indoors through an open window, especially in cold weather, or mounted outdoors on a suntracker. The whole instrument had to be moved and pointed toward the sun. The instrument housing was always shaded from direct sun, and the Teflon diffusor (entrance optics) was shaded between the scans. Among others, Adeyefa et al. (1997) have used the LI-1800 in this configuration for $\tau_{a,\lambda}$ determination, and, for example, Cachorro et al. (1987), Martínez-Lozano et al. (1998), and Jacovides et al. (2000) used the LI-1800 in a slightly different configuration.

The sun photometer was a three-channel Centre Suisse d'Electronique et de Microtechnique (CSEM) SPM2000, S/N 16 (CSEM2016 in the following), originally developed at the Physikalisch-Meteorologisches Observatorium Davos, Switzerland, World Radiation Center (hereinafter referred to as WRC). This instrument measures at approximately 368, 500, and 778 nm with 5-nm FWHM and 2.8° full-angle FOV. Each channel has a silicon photodiode detector with an integrated interference filter in a sealed housing assembled into a temperature-stabilized enclosure.

The broadband direct solar irradiance was measured with an Eppley Laboratory, Inc., normal incidence pyrheliometer (NIP) (No. 20919, 5.7° FOV).

b. Calibration

The LI-1800 was calibrated several times against standard lamps, which is the normal way to calibrate spectroradiometers of this type. The lines plotted in Fig. 1 represent the ratio of the spectral calibration factors derived at each calibration to the reference calibration factors, which simply were calculated as the mean of the four calibrations. The two standard lamps labeled SP-6 and SP-9 are 1000-W halogen free electron laser (FEL) lamps that were calibrated by the Swedish National Testing and Research Institute in June-1996, using the same reference that is traceable to the spectral irradiance scale of the National Institute of Standards and Technology. The total uncertainty in the calibration of the lamps is stated to be 2.5%–3.5% in the wavelength range of 300–1100 nm. Investigations by Kiedron et al. (1999) suggest that the uncertainty of the standard lamps could be even higher.

For wavelengths λ shorter than about 500 nm, the results of the calibration of the LI-1800 indicate a strong degradation in responsivity with time. For example, between the calibrations on 2 June 1999 and 22 October 1999, the responsivity at 368 nm decreased by almost 3.6%. For wavelengths in the range $369 \leq \lambda < 550$ nm, the change was smaller. For $\lambda < 368$ nm, the responsivity change was even larger. In the latter wavelength interval, the influence of noise is strong. To account for the change in responsivity of the LI-1800, the responsivity degradation for $\lambda < 550$ nm was modeled as a linear function of time and as a third-degree polynomial function of λ. Comparison with the CSEM2016 sun photometer 368-nm channel also supported the significant responsivity degradation with time of the LI-1800. For the same period (142 days), the degradation was estimated to be 2.4%, using CSEM2016 as reference.

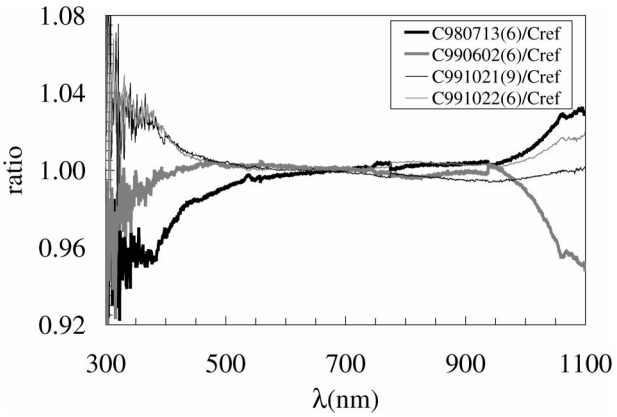

FIG. 1. Lamp calibrations of LI-1800: ratios of individual calibration results (spectral calibration factors) to the average of the results (Cref). The lamps are SP-6 and SP-9.

Also, for wavelengths longer than 950 nm, the calibration results varied considerably. However, there was not a continuous change over time. As already shown by Riordan et al. (1989), the LI-1800 has a very strong temperature dependence, especially in the IR region. Because neither the instrument nor the calibration room was temperature stabilized, the responsivity variations for $\lambda > 950$ nm are thought to be caused mainly by different detector temperatures. Because neither the LI-1800 was temperature stabilized nor was the detector temperature measured, the dependence on temperature was something for which one could not compensate. For determination of $\tau_{a,\lambda}$ at $\lambda > 950$ nm this drawback is serious. As a final calibration for $\lambda > 550$ nm, the average of the four lamp calibrations was applied to all LI-1800 measurements during the study. The uncertainty of LI-1800 irradiance measurements has been studied earlier (Myers 1989; Riordan et al. 1989).

For a sun photometer channel, the expected output voltage V_0 for a measurement outside the atmosphere at mean Sun–Earth distance is used as calibration constant. The CSEM2016 sun photometer has been calibrated several times at WRC, both against lamps and

by comparison with τ_a results from WRC's sun photometers at the wavelengths of CSEM2016. The difference between lamp and sun calibration results at WRC for CSEM2016 is 0%–4%. At wavelengths free from strong gaseous absorption, the so-called Langley calibrations of the WRC sun photometers are considered to be more accurate than lamp calibrations (Schmid and Wehrli 1995). To derive sun photometer V_0 from calibrations against the lamp requires knowledge about the extraterrestrial solar irradiance. Among others, the accuracy of calibrations against the lamp, therefore, depends on both the accuracy of the lamp and the accuracy of the extraterrestrial solar irradiance data used. Hence, the sun calibrations of the CSEM2016, using the Langley-calibrated WRC sun photometers as reference, are considered to be more accurate than the lamp calibrations. The CSEM2016 was compared with WRC's sun photometers in both February of 1998 and March of 1999. For some unknown reason, the resulting V_0 were 3%–4% higher in 1998 than in 1999 for all three channels.

The common way to calibrate reference sun photometers is through some type of Langley calibration method; see, for example, Schmid and Wehrli (1995). Through the use of a Langley calibration method, the exact knowledge of the extraterrestrial solar irradiance is not needed for the calculation of aerosol optical depth. Langley calibrations are preferably based on measurement data from a high-altitude site with very clean and stable atmospheric conditions, and this is how the WRC sun photometers are calibrated. However, as part of the quality control of the CSEM2016 measurements, analysis of classical Langley plots has also been made on data from the low-altitude site in Norrköping. In a classical Langley-plot calibration of one sun photometer channel, linear regression of the (natural) logarithm of the sun photometer signal, corrected to mean Sun–Earth distance, versus optical air mass is made. The point at which the regression line intercepts the ordinate yields the logarithm of V_0 for that particular channel. It is assumed that the optical depth is constant over the whole airmass range. There are several criteria defining a measurement period that is suitable for Langley-plot analysis. First, 1-min data from the sun photometer and collocated pyrheliometer were inspected manually to find candidate periods for Langley-plot analysis. Then, the basic objective criteria used here were as follows: approximate $\tau_{a,368} < 0.10$ (derived using $V_{0,368}$ from the latest calibration at WRC), optical air mass ≤ 7, range in optical air mass ≥ 3, and the difference between the regression line and accepted points of $\ln(V_{368}) < 0.2\%$ of $\ln(V_{368})$ at the highest accepted airmass value. The 368-nm channel is most sensitive to nonstable atmospheric (aerosol) conditions. After more than 30 V_0 values for each channel had been achieved in this way, outliers that were more than 5% off from the mean were discarded. In the end, about 80 occasions with accepted Langley-plot results were found during 1995–2001. The Norrköping Langley results indicate that the changes in sensitivity have been small in time for all of the CSEM2016 channels. The standard deviation of all accepted V_0 values were 2.0%, 1.4%, and 1.1% for the 368-, 500-, and 778-nm channels, respectively.

Linear regression of the V_0 results from Norrköping versus time agrees within 0.8% (778 nm) or better with the WRC sun calibration results of 1999, and they are about 3% lower than the WRC calibration of 1998. For this reason, the results of the 1999 WRC calibration were applied on all sun photometer data in this study. During September–October of 2000, the CSEM2016 also participated in the first filter radiometer comparison (FRC-I) held at WRC. The results of FRC-I indicate that 6–7 months after the last measurements of the current study were taken, the V_0 were 0.3%–1.3% higher than the ones used in this study. From this change, it is estimated that the uncertainty of the CSEM2016 V_0 is 2% at a level of confidence of 95% for all three channels.

The NIP 20919 is regularly calibrated against the two reference pyrheliometers of SMHI, PMO-6 absolute radiometer No. 811108 and Ångström pyrheliometer No. 171. The reference pyrheliometers participated in the three international pyrheliometer comparisons held between 1990 and 2000 at WRC and are directly traceable to the World Radiometric Reference. NIP 20919 has been found to be very stable over time, and a single calibration factor (111.0 W m^{-2} mV^{-1}) was adopted for the whole study. Every year several hundred calibration points are determined. The standard deviation of the individual NIP calibration results from one year is approximately 0.4% for all data and 0.3% for the cases in which the solar elevation was 35° or higher. The total uncertainty in the mean calibration constant originates mainly from the bias uncertainty of the reference pyrheliometers and is estimated to be 0.3% (1 standard deviation σ).

c. Calculation of aerosol optical depth

The calculations of $\tau_{a,\lambda}$ from the LI-1800 spectroradiometer measurements in the wavelength range of 360–1025 nm were further restricted, excluding portions affected by gaseous absorption bands of water vapor and oxygen (viz., 560–600, 616–666, 680–746, 754–774, 786–844, and 872–1014 nm; Adeyefa et al. 1997). Measurements in the range of 300–360 nm, where irradiance is considerably low, have been excluded because of the low signal-to-noise ratio in that region. At the remaining wavelengths, only the extinction due to Rayleigh scattering and ozone absorption were taken into account in the $\tau_{a,\lambda}$ calculations. The $\tau_{a,\lambda}$ at wavelength λ then becomes

$$\tau_{a,\lambda} = \ln\left(\frac{E_{0,\lambda}}{R^2 E_\lambda}\right) \Big/ m_a - \frac{m_R}{m_a}\frac{p}{p_0}\tau_{R,\lambda} - \frac{m_o}{m_a}\tau_{o,\lambda}, \quad (1)$$

where $E_{0,\lambda}$ is extraterrestrial solar irradiance at mean Sun–Earth distance, E_λ is measured direct solar irradi-

ance, R is actual Sun–Earth distance expressed in astronomical units, m_a is aerosol optical air mass, m_R is Rayleigh optical air mass (Kasten and Young 1989), m_o is ozone optical air mass (Robinson 1966), p is air pressure at station altitude, p_0 is standard pressure (=1013.25 hPa), $\tau_{R,\lambda}$ is Rayleigh optical depth [Fröhlich and Shaw (1980) with correction from Young (1980)], and $\tau_{o,\lambda}$ is ozone optical depth ($=l_o k_{o,\lambda}$, where l_o is total column amount of ozone and $k_{o,\lambda}$ is extinction coefficient for absorption in ozone). Because the spectroradiometer is calibrated to yield spectral irradiance, calculation of aerosol optical depth from the spectroradiometer measurements requires knowledge of the extraterrestrial solar spectrum. Data on the extraterrestrial solar irradiance and $k_{o,\lambda}$ were taken from the Simple Model of the Atmospheric Radiative Transfer of Sunshine (SMARTS2; Gueymard 1995), and data on total ozone were taken from collocated measurements with a Kipp and Zonen, Inc., Brewer MkIII spectroradiometer. Only one ozone value per day, measured close to local noon, was used. Because the vertical distribution of the aerosol particles was not known, the approximation $m_a = m_R$ was made.

For the sun photometer, values of $\tau_{a,\lambda}$ was calculated in the same way as for the LI-1800, except that $E_{0,\lambda}$ and E_λ in Eq. (1) were replaced by $V_{0,\lambda}$ and V_λ (=measured output voltage from λ-nm channel). The 500- and 778-nm channels were corrected for ozone absorption. No correction for nitrogen dioxide (NO_2) absorption was made.

Approximating solar radiation scattering and absorption by dust particles in the atmosphere as

$$\tau_{a,\lambda} = \beta\lambda^{-\alpha}, \tag{2}$$

with λ expressed in micrometers, was first introduced by Ångström (1929). Here, β is the aerosol optical depth at 1 μm, also known as Ångström's turbidity coefficient, and α is Ångström's wavelength exponent. This relation is utilized in several models to derive β from broadband direct solar irradiance measurements. In this study, the models presented by Grenier et al. (1994) and Gueymard (1998) are used. In both of these models, β is derived by assuming a constant value of the wavelength exponent, $\alpha = 1.3$. The models are based on parameterizations of the extinction processes that affect solar radiation transfer in a cloud-free atmosphere. Possible inputs to the models are solar position, (broad band or total) direct solar irradiance E_b, atmospheric water vapor content w, and air pressure. In the model by Gueymard, total columnar ozone and atmospheric NO_2 content could also be given as input. However, because constant values of ozone and NO_2 are used in the operational turbidity analysis at SMHI, the same restrictions were applied here on the $\tau_{a,\lambda}$ estimations from broadband measurements. The amounts of ozone and stratospheric and tropospheric NO_2 were held fixed at 0.35 atm cm, 0.1 matm cm, and 0.1 matm cm, respectively. The Ångström relation is then used to calculate $\tau_{a,\lambda}$ at the investigated wavelengths.

In many cases, using $\alpha = 1.3$ appears to be a good approximation. For the sun photometer data investigated in this study, the average α was found to be close to 1.3. This finding also holds for all data collected with the CSEM2016 between 1995 and 2001 at the same site. In these data (to be presented elsewhere), an annual cycle of monthly mean α, ranging from about 1.0 in winter to 1.6 in summer, is found. For the closest AERONET station on the island of Gotland in the Baltic Sea, 180 km from Norrköping, very similar results on α are found for level-2.0 data for March–November during 1999–2002. (These data are available online on the AERONET Web site at http://aeronet.gsfc.nasa.gov/.) Adeyefa et al. (1997) reported values on α of about 1.2 in conditions not affected by volcanic aerosol for the Abisko site in northernmost Sweden. Gonzi et al. (2002) investigated level-1.5 data from all available European AERONET stations. For most remote, urban, and coastal sites, the annual average α was between 1.0 and 1.6. Michalsky et al. (2001) report aerosol optical depth results from three sites in the United States. Also at these stations there is a typical annual cycle in α, with lower values in winter and higher values during summer. In conditions not influenced by volcanic aerosols, the mean annual variation is between approximately 1.0 and 1.6. Holben et al. (2001) also report monthly and yearly mean α values of between 1.0 and 1.6 at some AERONET stations, for example, in North and South America and in Europe. However, it is also clear that, for example, in pronounced oceanic and desert dust environments, α normally deviates considerably from 1.3.

One must keep in mind that the uncertainty in α determined from spectral aerosol optical depth data is significant. It is especially large in low-aerosol-optical-depth conditions. The resulting α is heavily dependent on calibration accuracy and the wavelength range that is used for its determination. In normal conditions, the smaller the wavelength range is, the higher the uncertainty becomes. Nevertheless, α is still commonly used to present a simple measure of the relative size distribution of the observed aerosol.

A correction of the original β model presented in the paper by Gueymard (1998) has been applied. The reason for this is the result obtained from a comparison between β values from Gueymard's original model and β derived with a minimization routine based on the complete SMARTS2 model. In the latter method, the difference between calculated and measured broadband direct irradiance was minimized for varying β input to SMARTS2. Calculations at more than 6000 data points of measured E_b and estimated w were compared. The approximate ranges in solar elevation, w, and β were 10°–57° ($m \approx 1.2$–5.6), 0.5–3.5 cm, and 0.005–0.350, respectively. The result of the comparison is shown in Fig. 2, where the difference between β derived from the minimization and β calculated with the parameterized

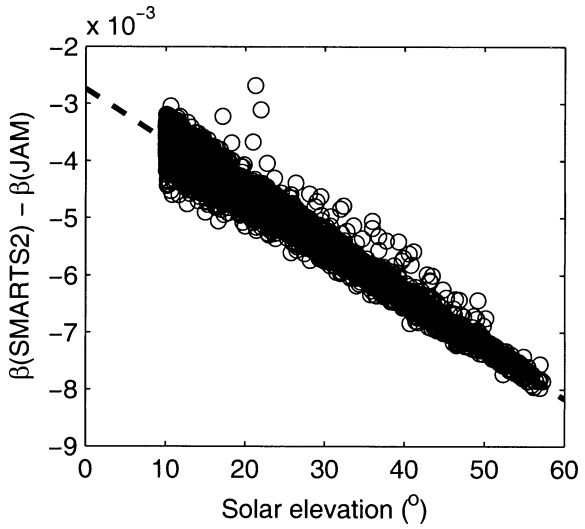

FIG. 2. The difference between β derived from minimization of SMARTS2 and β derived with the model by Gueymard (1998). The dashed line represents the linear correction function.

model of Gueymard (1998) is plotted against solar elevation. The SMARTS2 minimization always gives lower β values than does the model. It is apparent that the difference between the two methods is very close to a linear function of solar elevation. This disagreement is probably due to the parameterized turbidity model not being able to reproduce entirely the solar elevation dependence in SMARTS2 (C. A. Gueymard 2000, personal communication). Therefore, it is suggested that the β values from the original Gueymard model (β_{Gu}) should be corrected to

$$\beta = \beta_{\mathrm{Gu}} - 9.0 \times 10^{-5} h_a - 2.7 \times 10^{-3}, \qquad (3)$$

with h_a being apparent solar elevation in degrees. With this correction applied to β values given as input to the SMARTS2 model, the calculation of E_b agrees better with measured values. As will be shown below, estimates of spectral aerosol optical depth using the corrected β values also agree better with $\tau_{a,\lambda}$ derived from sun photometer measurements. Therefore, the corrected β values of the Gueymard model have been used in this study.

With the Gueymard model, it is also possible to compensate for the circumsolar radiation received by ordinary, relatively large FOV, pyrheliometers, such as the Eppley NIP. The circumsolar correction slightly increases the calculated β values. The solar elevation–corrected model, the original model, and the circumsolar-corrected original model were used to estimate spectral $\tau_{a,\lambda}$.

The column amount of water vapor w is a critical input for a good estimate of β. Here, two ways to calculate w have been tried. One way is to calculate w from the 6–12-h forecast fields of the operational weather-forecast High-Resolution Limited Area Model (HIRLAM). In a comparison of w calculated from upper-air sounding data and HIRLAM fields from April and July of 1997, it was found that, on average, w(HIRLAM) was higher than w(soundings). The difference was slightly less than 1 mm (=kg m^{-2}). It is not known how much water vapor there was above the highest points reached by the sounding balloons. The other way is to estimate w from the 2-m temperature and relative humidity according to the method by Gueymard (1994), hereinafter referred to as $w(T,$ RH).

d. Uncertainty of $\tau_{a,\lambda}$ derived from sun photometer measurements

According to the law of propagation of uncertainty, the combined standard uncertainty u_c of $y = f(x_1, x_2, \ldots, x_N)$ is

$$u_c(y) = \left[\sum_{i=1}^{N} \left(\frac{\partial f}{\partial x_i}\right)^2 u^2(x_l)\right]^{1/2} \qquad (4)$$

for independent input quantities x_i, where $u(x_i)$ is the standard uncertainty of each x_i (International Organization for Standardization 1995). To get the expanded uncertainty U, which is the uncertainty estimate valid at a certain level of confidence, u_c should be multiplied by a coverage factor k. For an approximate level of confidence of 95%, $k = 2$.

For determinations of $\tau_{a,\lambda}$ with Eq. (1) from sun photometer measurements, the (combined standard) uncertainty becomes

$$\begin{aligned} u_c(\tau_{a,\lambda}) = \Bigg\{ & \left[\frac{1}{m_a}\frac{u(V_{0,\lambda})}{V_{0,\lambda}}\right]^2 + \left[\frac{1}{m_a}\frac{u(V_{\mathrm{dir},\lambda})}{V_\lambda}\right]^2 + \left[\frac{1}{m_a}\frac{u(V_{\mathrm{dif},\lambda})}{V_\lambda}\right]^2 \\ & + \left[\frac{m_R}{m_a}u(\tau_{R,\lambda})\right]^2 + \left[\frac{m_o}{m_a}u(\tau_{o,\lambda})\right]^2 + \left[\frac{m_N}{m_a}u(\tau_{N,\lambda})\right]^2 \\ & + \left[\tau_{a,\lambda}\frac{u(m_a)}{m_a}\right]^2 + \left[\tau_{R,\lambda}\frac{u(m_R)}{m_a}\right]^2 + \left[\tau_{o,\lambda}\frac{u(m_o)}{m_a}\right]^2 \Bigg\}^{1/2} \end{aligned} \qquad (5)$$

for $p = p_0$ and $R = 1$ and neglecting uncertainties in these parameters as well as the contribution due to correlation among m_a, m_R, and m_o. Even though a sun photometer has a very small field of view, it will always see some scattered diffuse radiation in addition to the pure direct solar beam radiation. Therefore, the output voltage signal consists of contributions from both the direct beam $V_{\mathrm{dir},\lambda}$ and a small diffuse part $V_{\mathrm{dif},\lambda}$, so that $V_\lambda = V_{\mathrm{dif},\lambda} + V_{\mathrm{dif},\lambda}$. Absorption in NO_2 was not taken into account in the calculations of $\tau_{a,\lambda}$. The $[(m_N/m_a)u(\tau_{N,\lambda})]^2$ term, where $u(\tau_{N,\lambda})$ is the estimated optical depth of NO_2 absorption and m_N is the NO_2 air mass, must therefore be added in the uncertainty analysis. Uncertainty estimates similar to Eq. (5) were, for example, used by Russell et al. (1993) and Ingold et al. (2001).

The estimated expanded uncertainty of the calibration

is 2% at an approximate level of confidence of 95% ($k = 2$) for all three sun photometer channels. This uncertainty is considered to be normally distributed, and, therefore, the standard uncertainty is $u(V_{0,\lambda}) = 1\%$. Because $V_{\mathrm{dir},\lambda}$ is several orders of magnitude larger than $V_{\mathrm{dif},\lambda}$ under clear-sky conditions, when investigating $u(V_{\mathrm{dir},\lambda})$, $V_{\mathrm{dir},\lambda}$ is approximated by the total V_λ. Three sources of uncertainty are taken into account when estimating $u(V_{\mathrm{dir},\lambda})$. These are uncertainty of the voltmeter $u(V_\lambda)_{\mathrm{DVM}}$, uncertainty of the 1-min mean V_λ $u(V_\lambda)_{\mathrm{mi}}$, and uncertainty due to nonlinearity of the sun photometer, $u(V_\lambda)_{\mathrm{nl}}$. The total standard uncertainty of the voltage output is then calculated as

$$u(V_{\mathrm{dir},\lambda}) = [u(V_\lambda)^2_{\mathrm{DVM}} + u(V_\lambda)^2_{\mathrm{mi}} + u(V_\lambda)^2_{\mathrm{nl}}]^{1/2}. \quad (6)$$

From the voltmeter (Hewlett–Packard Company 3455A) manual, the uncertainty is stated to be ±(0.002% of range + 0.010% of reading). No information on the level of confidence for this uncertainty is provided. A rectangular distribution with the given uncertainty as semirange is assumed so that, $u(V_\lambda)_{\mathrm{DVM}} = (0.002\%\ \text{of range} + 0.010\%\ \text{of reading})/3^{1/2}$. The 1-min averages of V_λ are derived from $N = 10$ samples. The relative (experimental) standard deviation of the voltage readings $s(V_\lambda)$ has been investigated. It is normally calculated and stored in the measurement data files. When $s(V_\lambda)$ is not directly available from the measurement data, however, it was found that during clear skies $s(V_\lambda)$ could be estimated by the following simple linear function of m_a: $s(V_\lambda) = am_a + b$ (%), with $a = 0.14$, 0.04, and 0 and $b = 0.6$, 0.4, and 0.3 for the 368-, 500-, and 778-nm channels, respectively. To get the 1-min voltage uncertainty to a level of confidence of 95% $U_{95}(V_\lambda)_{\mathrm{mi}}$,

$$U_{95}(V_\lambda)_{\mathrm{mi}} = t_{95}(\nu)s(V_\lambda)/N^{1/2}(\%). \quad (7)$$

The factor $t_{95}(\nu) = 2.26$ is taken from the Student's t distribution for $\nu = N - 1 = 9$ degrees of freedom (see, e.g., International Organization for Standardization 1995). Last,

$$u(V_\lambda)_{\mathrm{mi}} = U_{95}(V_\lambda)_{\mathrm{mi}}/2 = t_{95}(\nu)s(V_\lambda)/2N^{1/2}\ (\%). \quad (8)$$

The silicon photodiodes in the sun photometer should be linear within 1% over a 6-decade range of input signals (Schmid et al. 1998). The nonlinearity over a 1-decade range is here assumed to be rectangularly distributed with 0.25% limits. Hence, the uncertainty in the voltage output from nonlinearity effects is modeled as

$$u(V_\lambda)_{\mathrm{nl}} = 0.25|\log_{10}(V_\lambda/V_{C,\lambda})|/3^{1/2}\ (\%), \quad (9)$$

where $V_{C,\lambda}$ is the approximate mean output voltage during calibration of the sun photometer at WRC.

The diffuse radiation seen by the sun photometer was investigated with the SMARTS2 model, using fixed values of the input variables of single scattering albedo = 0.95, aerosol asymmetry parameter = 0.8, altitude = 0 m, instrument half view angle = 1.4°, FWHM = 5 nm, and Ångström's wavelength exponent = 1.3, for the midlatitude summer atmosphere. It turned out that, for constant $\tau_{a,\lambda}$, $u(V_{\mathrm{dif},\lambda})/V_\lambda$ increased linearly with m_a. When instead keeping m_a constant, $u(V_{\mathrm{dif},\lambda})/V_\lambda$ increased almost linearly with $\tau_{a,\lambda}$. As opposed to the results of more thorough investigations by Russell et al. (1993), the effect of diffuse radiation did vary only very little with wavelength according to the SMARTS2 simulations. Here, the relative voltage uncertainty from the diffuse radiation seen by the photometer is modeled as

$$u(V_{\mathrm{dif},\lambda}) = m_a(12\tau_{a,\lambda} + 0.1)/14\ (\%). \quad (10)$$

In conditions with similar aerosol optical depth spectra, as of this study ($\alpha \approx 1.3$), this produces significantly higher $u(\tau_{a,\lambda})/\tau_{a,\lambda}$ values due only to diffuse light (by approximately a factor of 2) than were reported by Russell et al. (1993) for their measurements at the Mauna Loa, Hawaii, Observatory (MLO), 3.4-km altitude. At a near–sea level site, $u(\tau_{a,\lambda})/\tau_{a,\lambda}$ should be higher than at MLO because of stronger Rayleigh scattering. In comparison with the results by Russell et al. (1993), it is still more likely that the uncertainty from diffuse radiation is here overestimated instead of being underestimated.

The uncertainty in Rayleigh optical depth $\tau_{R,\lambda}$ is stated to be within 0.7% (Fröhlich and Shaw 1980). Young (1980) found that the Fröhlich and Shaw formula for $\tau_{R,\lambda}$ was erroneous and suggested a correction. At 368 and 500 nm, $\tau_{R,\lambda}$ calculated by the corrected Fröhlich and Shaw formula differs by ≤0.1% from $\tau_{R,\lambda}$ calculated by a newer parameterization in Bodhaine et al. (1999). At 778 nm, the difference is <0.25%. Therefore, assuming ±0.7% as the limits of a rectangular uncertainty interval for $\tau_{R,\lambda}$ is believed not to be an underestimation. Thus,

$$u(\tau_{R,\lambda}) = 0.007\tau_{R,\lambda}/3^{1/2}. \quad (11)$$

The uncertainty in ozone optical depth originates from uncertainty in atmospheric ozone amount and uncertainty in the absorption coefficients. The total ozone is taken from the measurements with the Brewer spectroradiometer, which produces very accurate ozone data. However, only daily values of total ozone are used in the calculations of $\tau_{a,\lambda}$. From analysis of the day-to-day variation and uncertainty in measurements, the standard uncertainty in total ozone is estimated to 15 Dobson units, or 5%. The standard uncertainty of the (temperature dependent) ozone absorption coefficients used in SMARTS2 is estimated to be 10%. The standard uncertainty of ozone optical depth is, therefore, approximated to $(5^2 + 10^2)^{1/2} \approx 11\%$, so that

$$u(\tau_{o,\lambda}) = 0.11\tau_{o,\lambda}. \quad (12)$$

The amount of NO_2 in the atmosphere over the measuring site is unknown. In many model reference atmospheres, the total column NO_2 is about 2×10^{-4} atm cm (Gueymard 1995). Van Roozendael et al. (1997) report on columnar measurements of NO_2 at two European sites with low background NO_2 content in the troposphere. At these sites, monthly values of NO_2

varies between about 1×10^{15} molecules cm^{-2} ($=0.4 \times 10^{-4}$ atm cm) in winter and 7×10^{15} molecules cm^{-2} ($=2.6 \times 10^{-4}$ atm cm) in summer. To calculate the standard uncertainty in NO_2 optical depth $u(\tau_{N,\lambda})$, the NO_2 absorption coefficients $k_{N,\lambda}$ of SMARTS2 were multiplied by 2×10^{-4} atm cm NO_2; that is,

$$u(\tau_{N,\lambda}) = 2 \times 10^{-4} k_{N,\lambda}. \quad (13)$$

The assumption is that uncertainty in both NO_2 amount and absorption coefficients is covered by this estimate.

Not taking NO_2 absorption and diffuse radiation into account introduces biases in the derived $\tau_{a,\lambda}$ values. However, these biases are of different sign and therefore cancel out each other to some extent, at least at the wavelengths of 368 and 500 nm.

Standard uncertainty of Rayleigh optical air mass $u(m_R)$ originates mainly from uncertainty in the formula for m_R, inaccuracy of data acquisition clock, uncertainty in calculated solar elevation without refraction, and uncertainty in refraction. The deviation of the m_R formula from detailed calculations of specific atmospheric conditions is very small, $\leq$0.065% for $m_R \leq 7$ (Kasten and Young 1989). The error of the data acquisition clock was always $<$5 s. The Astronomical Almanac algorithm for calculation of solar elevation is accurate within 0.01° (Michalsky 1988). For air masses $\leq$7, the correction for refraction is considered to be accurate within $\pm$0.03° in 95% of the cases in this study. Hence, the expanded uncertainty in Rayleigh optical air mass is calculated as $U_{95}(m_R) = m_R(h_a - 0.04) - m_R(h_a)$, with h_a being apparent solar elevation. This should cover the uncertainty in m_R at a level of confidence of $\geq$95%, that is, $k = 2$, thus giving

$$u(m_R) = [m_R(h_a - 0.04) - m_R(h_a)]/2. \quad (14)$$

The ozone optical air mass is calculated using a default mean ozone layer height $z_o = 22$ km. Only the uncertainty in ozone layer height is taken into account when estimating the uncertainty in the ozone optical air mass, $u(m_o)$. This uncertainty is estimated to

$$u(m_o) = [m_o(z_o = 16 \text{ km}) - m_o(z_o = 22 \text{ km})]/2. \quad (15)$$

In the calculations of aerosol optical depth, m_a was set equal to m_R. Often, in SMARTS2, for example, the vertical aerosol particle distribution is assumed to be more concentrated near the ground than the vertical distribution of the molecules of the air, leading to $m_a > m_R$. This is probably a good assumption in situations without volcanic aerosols in the stratosphere. The uncertainty in m_a from unknown vertical particle distribution is here calculated as

$$u[m_a(\text{vert distr.})] = k_a[m_a(\text{SMARTS2}) - m_R], \quad (16)$$

with $k_a = 0.75$. The uncertainty of calculated apparent solar elevation is accounted for in the same way as for m_R. Thus,

$$u[m_a(h_a)] = [m_a(\text{SMARTS2}, h_a - 0.04) - m_a(\text{SMARTS2}, h_a)]/2. \quad (17)$$

Last, the combined standard uncertainty of m_a is given by

$$u(m_a) = \{u[m_a(\text{vert. distr.})]^2 + u[m_a(h_a)]^2\}^{1/2}. \quad (18)$$

The magnitude of the estimated total uncertainty (expanded uncertainty with coverage factor $k = 2$) of $\tau_{a,\lambda}$, as well as the contributions from the individual sources of uncertainty considered here, is plotted versus aerosol optical air mass in Fig. 3. To show their contribution to the total uncertainty, the individual standard uncertainties are multiplied by $k = 2$. The individual uncertainties are here assumed to be symmetrically distributed around zero. It is evident that for $m_a \leq 3$ the accuracy of the calibration of the sun photometer is the most important source of uncertainty at all wavelengths. At higher air masses, especially for relatively high $\tau_{a,\lambda}$, the uncertainty in m_a is the largest source of uncertainty. It is hoped that the uncertainty in m_a is here somewhat overestimated. In situations without any significant amount of volcanic aerosol particles in the stratosphere, the uncertainty could probably be reduced by not taking $m_a = m_R$ and instead using m_a(SMARTS2), for example.

So far it has been assumed that the probability functions of the individual uncertainties are normally or rectangularly distributed around zero. However, this is not the case in reality for some of the sources of uncertainty. The diffuse radiation seen by a direct sun radiometer only tends to reduce the derived aerosol optical depths. On the other hand, neglecting NO_2 absorption results in overestimated values of $\tau_{a,\lambda}$. The same holds for using a too-small value of m_a, which is the case if m_a really is more close to m_a(SMARTS2) than to m_R. For these reasons, the positive and negative uncertainty limits are calculated separately. In the estimated positive (upper) uncertainty limits (see Fig. 6), no $u(\tau_{N,\lambda})$ was taken into account and only 1/3 of $u(m_a)$ was considered. It was simply considered very unlikely that m_a was actually lower than m_R by more than 2×0.75 [m_a(SMARTS2) $- m_R$]/3 (95% level of confidence) under the measuring conditions during this study, with no, or only very small, amounts of volcanic aerosol particles in the stratosphere. In the estimated negative (lower) uncertainty limits, no $u(V_{\text{dif},\lambda})$ was taken into account. The asymmetry of the uncertainty estimates is, however, only visible at high values of m_a (see Fig. 6).

According to the International Organization of Standardization (1995), a standard uncertainty is classified as either being obtained from statistical analysis, a type-A evaluation of standard uncertainty, or being obtained by means other than statistical analysis, a type-B evaluation of standard uncertainty. In this study, only two of the individual standard uncertainties, $u(V_\lambda)_{\text{DVM}}$ and $u(V_\lambda)_{\text{mi}}$, are obtained by statistical analysis (type A). All of the other uncertainties were instead obtained by means other than statistical analysis (type B). In all

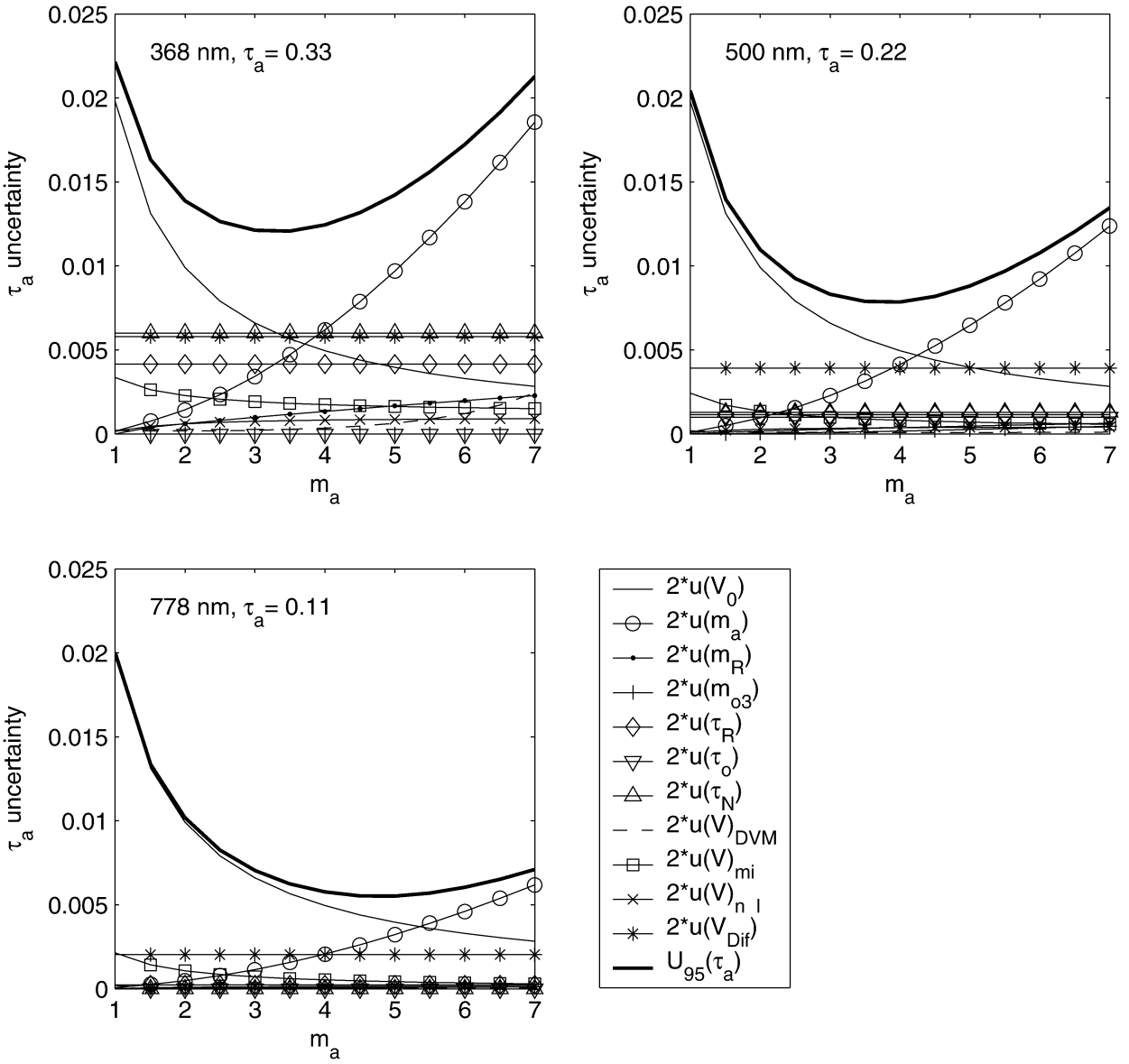

FIG. 3. Expanded uncertainty ($k = 2$) of aerosol optical depth $U_{95}(\tau_a)$ and the effects of individual sources of uncertainty on the uncertainty of $\tau_{a,\lambda}$ derived from CSEM2016 sun photometer measurements at 368, 500, and 778 nm.

TABLE 1. Measuring conditions during the study: $\tau_{a,\lambda}$, α, and β are calculated from the sun photometer CSEM2016 data, and w is calculated from HIRLAM.

	m_a	w (cm)	$\tau_{a,368}$	$\tau_{a,500}$	$\tau_{a,778}$	α	β
Mean	2.52	1.08	0.115	0.073	0.037	1.377	0.028
Median	2.17	0.96	0.084	0.054	0.029	1.381	0.022
Max	6.69	2.70	0.428	0.292	0.155	1.940	0.113
Min	1.23	0.31	0.026	0.017	0.008	0.604	0.008
(Std dev)	1.15	0.49	0.087	0.057	0.028	0.241	0.020

cases, the type-B uncertainty evaluations were assumed to have infinite degrees of freedom. [See the International Organization of Standardization (1995) for details on evaluation and expression of uncertainty in measurements.]

3. Results

The measuring and aerosol conditions during this study (March 1999–March 2000), as determined by CSEM2016, are listed in Table 1. Statistics of the $\tau_{a,\lambda}$ comparison are summarized in Tables 2 and 3. As is clear from Table 1, the atmospheric turbidity and $\tau_{a,\lambda}$ were mostly low during the study, with no occasions of really high turbidity ($\beta \geq 0.200$).

TABLE 2. Difference in $\tau_{a,\lambda}$ between LI-1800 spectroradiometer and CSEM2016 sun photometer, and between broadband method (NIP) and CSEM2016. Comparison statistics are based on 279 cases. SEC = solar elevation correction of β according to Eq. (3). Orig = original model of β by Gueymard. OrigCS = original model of β with correction for circumsolar irradiance by Gueymard.

	368-nm LI-1800	368-nm NIP SEC	368-nm NIP Orig	368-nm NIP OrigCS	500-nm LI-1800	500-nm NIP SEC	500-nm NIP Orig	500-nm NIP OrigCS	778-nm LI-1800	778-nm NIP SEC	778-nm NIP Orig	778-nm NIP OrigCS
Mean	0.024	0.014	0.034	0.040	−0.004	0.014	0.027	0.031	−0.002	0.013	0.020	0.022
Median	0.022	0.015	0.035	0.040	−0.003	0.014	0.026	0.029	−0.001	0.013	0.021	0.023
Max	0.077	0.074	0.099	0.107	0.005	0.049	0.066	0.071	0.005	0.028	0.039	0.041
Min	−0.004	−0.057	−0.038	−0.026	−0.024	−0.017	−0.004	0.003	−0.014	−0.004	0.002	0.003
Rms	0.029	0.028	0.042	0.047	0.006	0.019	0.030	0.034	0.005	0.014	0.021	0.023
Std dev	0.016	0.024	0.025	0.025	0.004	0.013	0.014	0.014	0.004	0.006	0.006	0.007

Examples of instantaneous spectral $\tau_{a,\lambda}$ derived using the three different instruments are plotted versus wavelength in log–log diagrams in Fig. 4. The $\tau_{a,\lambda}$ values are from one very clear day (29 April 1999) and from a more turbid day (14 September 1999). For the more turbid case, the Ångström relation is a very good approximation of the spectral distribution of $\tau_{a,\lambda}$ ($\alpha = 1.7$, $\beta = 0.025$), according to both the spectroradiometer and the sun photometer. Using single α and β in the clear case still appears to be a good approximation for the CSEM2016 $\tau_{a,\lambda}$ values ($\alpha = 1.2$, $\beta = 0.015$). However, this is not the case for the LI-1800 results. The log–log plot could be misleading, but, nevertheless, the disagreement between LI-1800 and CSEM2016 $\tau_{a,\lambda}$ for $\lambda < 450$ nm and $\lambda > 950$ nm is much higher in the clear case. The LI-1800 $\tau_{a,\lambda}$ data at these wavelengths are most probably influenced by measurement errors.

In addition to the temperature dependence for $\lambda > 950$ nm and the presumed responsivity degradation with time (or exposure?) for $\lambda < 500$ nm in the LI-1800, an airmass dependence at shorter wavelengths is indicated by comparison with the CSEM2016 at 368 nm. Using the sun photometer as reference, calibration constants for the LI-1800 at 368 nm, which would give the same $\tau_{a,\lambda}$ as the CSEM2016, were calculated. LI-1800 calibration factors for $\lambda = 368$ nm appear to be very dependent on air mass (Fig. 5). Possible explanations for this result could be nonlinearity, temperature dependence, and tilting of the instrument. Of course, an erroneous $V_{0,368}$ applied on the CSEM2016 signals could also lead to such a result. However, it is strongly believed that the error in $V_{0,368}$ (plus nonlinearity in V_{368}) is much less than the 10% that at least is needed to give results similar to those in Fig. 5. If such a large change had occurred after the calibration of CSEM2016 in 1999 at WRC, it would have shown up at FRC-I or even in the Langley plots of sun photometer data from Norrköping. After the calibration in Davos, 35 accepted Langley plots have been made. The maximum deviation from the average $V_{0,368}$ is about ±4%, but the deviation of the mean from the WRC $V_{0,368}$ is only +0.3%.

The $\tau_{a,\lambda}$-weighted averages of $U_{95}(\tau_{a,\lambda})$ estimated for each value of $\tau_{a,\lambda}$(CSEM2016) were only 0.014, 0.011, and 0.011. There are no significant deviations from these values when looking at the positive and negative uncertainty limits separately at 500 and 778 nm. At 368 nm, the positive and negative uncertainty limits were calculated to +0.012 and −0.013. These low uncertainties are partly due to the mostly low $\tau_{a,\lambda}$ values and the large number of measurements with m_a in the range between 2 and 5 during the study. By taking the average uncertainty as the uncertainty of the average or median aerosol optical depth, it is assumed that all individual standard uncertainties $u(x_i)$ are made up of bias uncertainty only. Indeed, the major part of many of the standard uncertainties, such as $u(V_{0,\lambda})$, for example, is really bias uncertainty. However, among others, depending on the considered timescale, minor or major parts of all standard uncertainties are of random nature. Ignoring this fact does at least not lead to an underestimation of the uncertainty of the average $\tau_{a,\lambda}$ results.

The differences in aerosol optical depth derived from

TABLE 3. Differences in aerosol optical depth derived from pyrheliometer measurements according to Grenier et al. and from sun photometer measurements. Two different water vapor inputs to the broadband method were used.

	368-nm $\beta[w(H)]$*	368-nm $\beta[w(T, \text{RH})]$**	500-nm $\beta[w(H)]$	500-nm $\beta[w(T, \text{RH})]$	778-nm $\beta[w(H)]$	778-nm $\beta[w(T, \text{RH})]$
Mean	0.044	0.055	0.035	0.041	0.008	0.028
Median	0.044	0.050	0.032	0.036	0.011	0.027
Max	0.108	0.151	0.072	0.087	0.028	0.059
Min	−0.007	0.000	0.005	0.012	−0.026	0.008
Rms	0.050	0.062	0.037	0.045	0.013	0.030
Std dev	0.023	0.029	0.013	0.018	0.010	0.011

* $\beta[w(H)]$ = columnar water vapor calculated from HIRLAM.
** $\beta[w(T, \text{RH})]$ = columnar water vapor calculated from 2-m temperature and relative humidity.

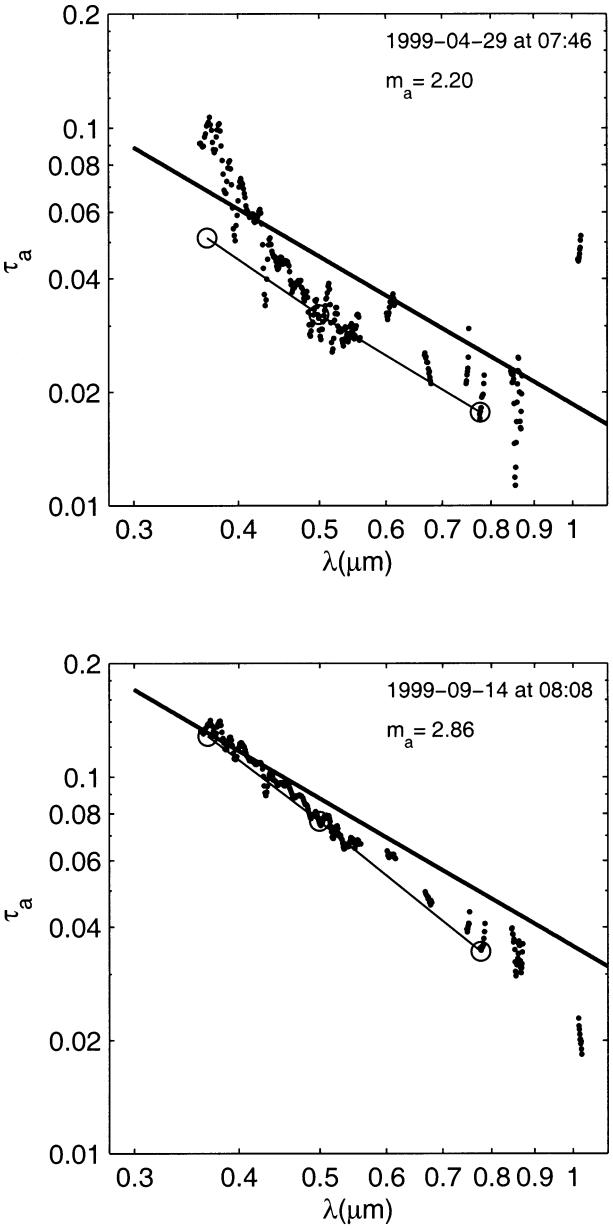

FIG. 4. Examples of spectral τ_a derived from measurements with LI-1800 (dots), CSEM2016 (circle-line), and NIP with corrected β model by Gueymard (full line).

sun photometer measurements and the two other methods for the three investigated wavelengths are plotted vs optical air mass in Fig. 6. Also, the uncertainty in sun photometer $\tau_{a,\lambda}$, at an approximate level of confidence of 95% is shown. The uncertainty is calculated for 0.33, 0.22, and 0.11 aerosol optical depth for 368-, 500-, and 778-nm wavelengths, respectively. In at least 95% of the cases, $\tau_{a,\lambda}$ were equal to or lower than these limits. These limits are significantly higher than the average and median values of $\tau_{a,\lambda}$ for the whole study (see Table 1). The total number of cases is 279, originating from 32 days spread over 1 yr. For $m_a > 2$, the agreement between the

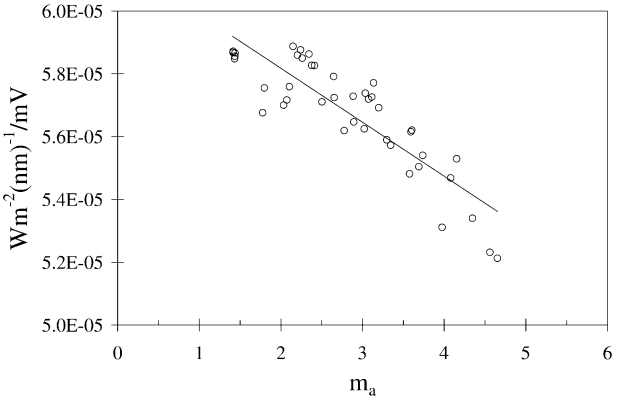

FIG. 5. Calibration factors for LI-1800 at 368 nm using CSEM2016 as reference, 27–29 Apr 1999.

LI-1800 and the CSEM2016 $\tau_{a,\lambda}$ determinations is good, normally within 0.01, at 500 and 778 nm (Fig. 6). At 368 nm the difference is larger, especially for $m_a < 3$, and the dependence on optical air mass is also clear. Because of the problems of the LI-1800 at shorter wavelengths, the mean and rms differences in aerosol optical depth at 368 nm are actually larger between the two spectral instruments than between the pyrheliometer [$\tau_{a,\lambda}$(NIP)] and the sun photometer retrievals (Fig. 6 and Table 2).

In most cases, the broadband methods slightly overestimate $\tau_{a,\lambda}$ at all three wavelengths. For the best broadband method in this comparison, the solar elevation–corrected [Eq. (3)] Gueymard model without circumsolar compensation, and using w(HIRLAM) as precipitable water input, the $\tau_{a,\lambda}$(NIP) estimates were on average 0.014, 0.014, and 0.013 higher than the sun photometer $\tau_{a,\lambda}$ values at 368, 500, and 778 nm, respectively. This result is close to, but just above, the average uncertainty of the sun photometer $\tau_{a,\lambda}$ values. Considering the uncertainties involved with the broadband method, the agreement in average aerosol optical depth between sun photometer and the pyrheliometer method is surprisingly good. Using the original model by Gueymard, but still without the circumsolar compensation, increased the mean differences to 0.034, 0.027, and 0.020, respectively. Because these results are already too high, also adding the proposed circumsolar correction to the original model increased the mean differences even further, to 0.040, 0.031, and 0.022 for the same wavelengths (Table 2). When considering these latter differences, it must be kept in mind that the sun photometer optical depths were not corrected for circumsolar radiation. The circumsolar contribution was only included in the uncertainty analysis. The quality of the circumsolar correction of β by Gueymard cannot be evaluated from the results of this study.

As mentioned above, $m_a = m_R$ in the calculations of $\tau_{a,\lambda}$(CSEM2016) and $\tau_{a,\lambda}$(LI-1800). This is not the case in the broadband method, where m_a is calculated as proposed by Gueymard (1998). If the same values on

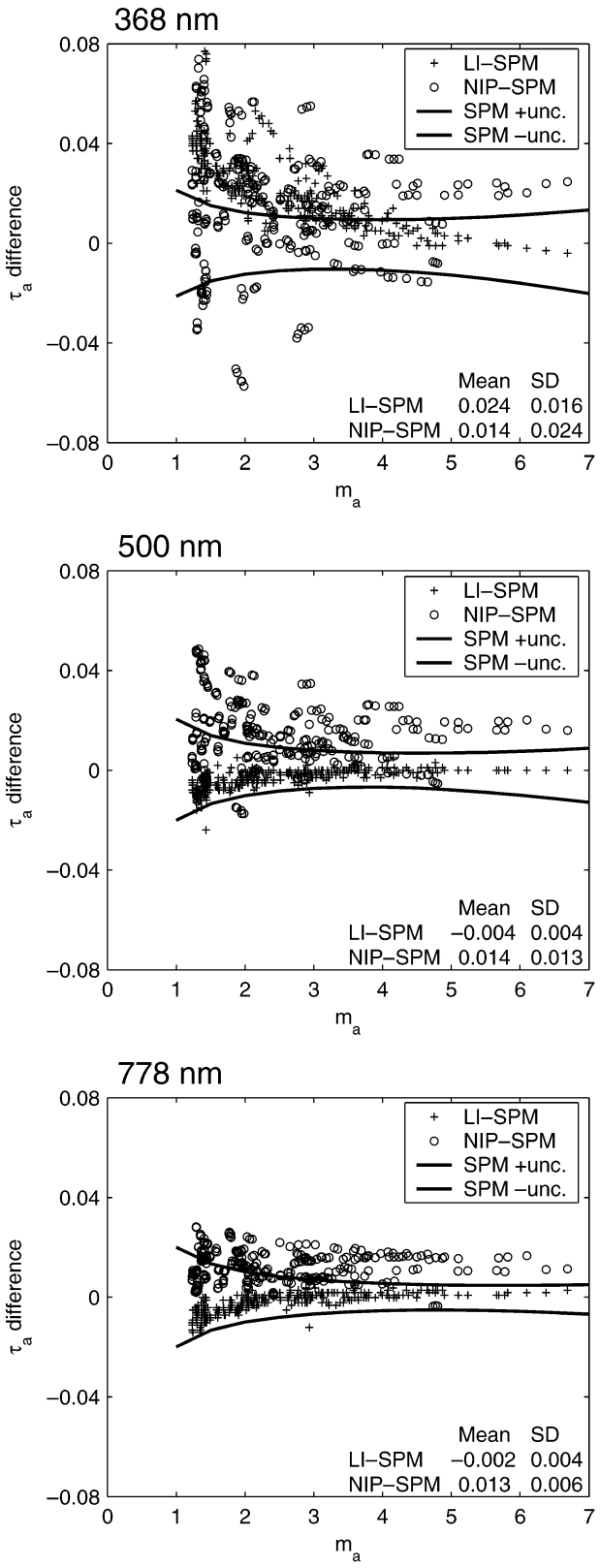

FIG. 6. Differences in derived $\tau_{a,\lambda}$ at 368, 500, and 778 nm, and uncertainty limits for $\tau_{a,\lambda}$(SPM): LI = LI-1800 spectroradiometer, NIP = pyrheliometer, SPM = CSEM2016 sun photometer.

m_a had been used in both the spectral and broadband methods, the $\tau_{a,\lambda}$ differences would have been slightly larger, especially for high m_a.

For the same water vapor amount, w(HIRLAM), $\tau_{a,\lambda}$(NIP) estimated from the β model by Grenier et al. (1994) are on average slightly higher than those of the original Gueymard model at 368 and 500 nm. At 778 nm it is slightly lower but still exceeds the sun photometer $\tau_{a,\lambda}$ values (Table 3). There are only minor differences in the scatter between the two broadband methods (standard deviation in Tables 2 and 3).

There is naturally a larger scatter in the difference between $\tau_{a,\lambda}$ derived from pyrheliometer and spectral (sun photometer) measurements (Fig. 6). This scatter is mainly due to erroneous values of α and w used in the broadband method. The scatter in $\tau_{a,\lambda}$ differences appears to decrease with increasing air mass. The errors introduced in β by using incorrect values of w and total ozone decrease marginally with increasing air mass. It is thought that the main reason why the scatter in $\tau_{a,\lambda}$ differences in Fig. 6 decreases with increasing air mass is simply the fact that the range in atmospheric conditions was small for the measurements when m_a was high. For example, the values of α for the 10 cases with $m_a > 5$ only varied between 1.2 and 1.5.

The importance of a good estimate of w to be used when estimating β is illustrated in Table 3. On average, $w(T, \text{RH})$ was found to be lower by 0.17 cm than w(HIRLAM), resulting in higher values of β and $\tau_{a,\lambda}$. However, the $w(T, \text{RH}) - w$(HIRLAM) difference ranges from largely positive (0.86 cm) to largely negative (−1.28 cm). According to the $\tau_{a,\lambda}$ difference statistics in Table 3, using w(HIRLAM) significantly improves the $\tau_{a,\lambda}$(NIP) estimates.

4. Conclusions and discussion

From this study, the following conclusions are drawn:

1) According to the CSEM2016 sun photometer, an average $\alpha = 1.38$ (in the wavelength range of 368–778 nm) was found during the period of the study at the inland site in southern Sweden. Hence, using $\alpha = 1.3$ in the $\tau_{a,\lambda}$ determinations from broadband measurements is fairly well supported.
2) In general, estimates of spectral $\tau_{a,\lambda}(\lambda < 1000$ nm) from pyrheliometer measurements of the direct irradiance using the β models by Grenier et al. (1994) and Gueymard (1998) were found to exceed $\tau_{a,\lambda}$ as determined from accurate sun photometer measurements. Average results of the β model by Gueymard without circumsolar compensation but corrected according to Eq. (3) are closest to the reference values but still slightly exceed the estimated measurement uncertainty of the sun photometer $\tau_{a,\lambda}$ values.
3) Taking precipitable water amount from an atmospheric model results in significantly better turbidity

estimates than if w is calculated from measured 2-m temperature and relative humidity.

4) The two largest sources of uncertainty in aerosol optical depth derived from sun photometer measurements are uncertainties of calibration and aerosol optical air mass.
5) Especially because of its low accuracy and instability at $\lambda < 500$ nm and $\lambda > 950$ nm, the LI-1800, in its current configuration, is not suited well for determination of $\tau_{a,\lambda}$ and its spectral dependence in the form of Ångström's wavelength exponent α. In particular, it is not suited for long-term monitoring and/or at locations where the turbidity normally is low.

As long as there are no major errors in the WRC calibration of the CSEM2016 or in the NIP calibration, it appears certain that $\tau_{a,\lambda}(\lambda < 1000$ nm) is overestimated with the broadband methods. Considering the uncertainties involved with the broadband method, however, the agreement in average aerosol optical depth between sun photometer and the closest pyrheliometer method is considered to be very good. Molineaux et al. (1998) compared aerosol optical depth at 700 nm derived from spectral and broadband measurements. For a 9-month period in Geneva, Switzerland, they found mean differences ranging from -0.09 to 0.033 in aerosol optical depth at 700 nm between broadband and spectral methods. In the majority of cases, the broadband methods gave higher optical depths. The differences depended on the aerosol model used, the calibration of the spectral instrument, and how the columnar water vapor was derived. The standard deviations were about the same as or slightly higher than what was found for the 500-nm wavelength in this study.

It was indicated that w(HIRLAM) values used on average could be a little too high. Giving lower w as input, higher β [and higher $\tau_{a,\lambda}(\lambda < 1000$ nm)] will be returned by the turbidity models, as was the case with $w(T,$ RH). From sensitivity calculations with SMARTS2, it turned out that 10%–15% higher w(HIRLAM) values would be needed to remove fully the average differences between CSEM2016 $\tau_{a,\lambda}$ and $\tau_{a,\lambda}$ from the corrected Gueymard method. It can not be excluded that w(HIRLAM) actually was negatively biased by this amount. More validation of w from 6–12-h forecast fields of HIRLAM needs to be done to assess better this source of uncertainty. It is not known how large an impact the errors in the calculated water vapor coefficients and their parameterization in the broadband turbidity models could have on the derived β and aerosol optical depths.

If a higher α of 1.38 had been used in the development of the β models, this would have led to even higher $\tau_{a,\lambda}$ at 368 and 500 nm and negligibly lower $\tau_{a,\lambda}$ at 778 nm in the end. If the CSEM2016 wavelength pairs 368/500 nm and 500/778 nm were considered separately, the average value of α would be determined to 1.54 and 1.25, respectively. If these α values had been used in the Gueymard model in the wavelength ranges <500 nm and >500 nm, respectively, which is possible with the SMARTS2 model, the broadband method $\tau_{a,\lambda}$ would have increased by approximately 0.010 at 368 nm and decreased by approximately 0.003 at 500 nm for the data used in the study. The 778-nm mean $\tau_{a,\lambda}$ would have been practically unaffected.

Broadband measurements certainly cannot replace spectral measurements for determination of aerosol optical depth. This study suggests that at locations at which only direct solar irradiance measurements are made, one can still get fairly good estimates of the average aerosol optical depth conditions by applying a broadband turbidity model on the direct irradiance data. If the direct irradiance measurements cannot be made close to an upper-air station, the needed columnar water vapor input should be derived from a numerical weather analysis or prediction model.

In pronounced oceanic environments (e.g., Wilson and Forgan 2002) or in places commonly affected by desert dust or biomass-burning aerosols (e.g., Eck et al. 1999; Holben et al. 2001), as well as after major volcanic eruptions (e.g., Dutton et al. 1994; Kaufman et al. 1994; Michalsky et al. 2001), the spectral dependence of aerosol optical depth is known to deviate significantly from the simple Ångström relation with $\alpha = 1.3$, as assumed in the published broadband turbidity methods. The turbidity models should, for these places and/or times, be modified to represent more closely the aerosol optical depth dependence on wavelength.

The atmospheric conditions during the study were mostly very clear and dry in a global perspective. This fact has to be accounted for when considering the representativity of the aerosol optical depth comparison.

Acknowledgments. The authors are grateful to C. Gueymard for providing the SMARTS2 code. The work has been carried out with financial support from the Swedish National Space Board, which is gratefully acknowledged.

REFERENCES

Adeyefa, Z. D., B. Holmgren, and J. A. Adedokun, 1997: Spectral solar radiation measurements and turbidity: Comparative studies within a tropical and a sub-arctic environment. *Sol. Energy,* **60,** 17–24.

Ångström, A., 1929: On the atmospheric transmission of sun radiation and on dust in the air. *Geogr. Ann.,* **2,** 156–166.

Bodhaine, B. A., N. B. Wood, E. G. Dutton, and J. R. Slusser, 1999: On Rayleigh optical depth calculations. *J. Atmos. Oceanic Technol.,* **16,** 1854–1861.

Cachorro, V. E., A. M. de Frutos, and J. L. Casanova, 1987: Determination of the Ångstrom parameters. *Appl. Opt.,* **26,** 3069–3076.

Dutton, E. G., P. Reddy, S. Ryan, and J. J. DeLuisi, 1994: Features and effects of aerosol optical depth observed at Mauna Loa, Hawaii: 1982–1992. *J. Geophys. Res.,* **99,** 8295–8306.

Eck, T. F., B. N. Holben, J. S. Reid, O. Dubovik, A. Smirnov, N. T. O'Neill, I. Slutsker, and S. Kinne, 1999: Wavelength dependence of the optical depth of biomass burning, urban and desert dust aerosols. *J. Geophys. Res.,* **104,** 31 333–31 349.

Fröhlich, C., and G. E. Shaw, 1980: New determination of Rayleigh scattering in the terrestrial atmosphere. *Appl. Opt.,* **19,** 1773–1775.

Gonzi, S., D. Baumgartner, and E. Putz, 2002: Aerosol climatology and optical properties of key aerosol types observed in Europe. Institute for Geophysics, Astrophysics, and Meteorology, University of Graz Tech. Rep. for EU 1/2002, 52 pp. [Available online at http://www.muk.uni-hannover.de/~martin/results/deliverables/1.5/b.pdf.]

Grenier, J. C., A. de la Casiniere, and T. Cabot, 1994: A spectral model on Linke's turbidity factor and its experimental implications. *Sol. Energy,* **52,** 303–313.

Gueymard, C., 1994: Analysis of monthly average atmospheric precipitable water and turbidity in Canada and northern United States. *Sol. Energy,* **53,** 57–71.

——, 1995: SMARTS2, a Simple Model for the Atmospheric Radiative Transfer of Sunshine: Algorithms and performance assessment. Florida Solar Energy Center Tech. Rep. FSEC-PF-270-95, 78 pp. [Available from Florida Solar Energy Center, 1679 Clearlake Rd., Cocoa, FL 32922–5703.]

——, 1998: Turbidity determination from broadband irradiance measurements: A detailed multicoefficient approach. *J. Appl. Meteor.,* **37,** 414–435.

Holben, B. N., and Coauthors, 1998: AERONET—A federated instrument network and data archive for aerosol characterization. *Remote Sens. Environ.,* **66,** 1–16.

——, and Coauthors, 2001: An emerging ground-based aerosol climatology: Aerosol optical depth from AERONET. *J. Geophys. Res.,* **106,** 12 067–12 097.

Ingold, T., C. Mätzler, and N. Kämpfer, 2001: Aerosol optical depth measurements by means of a sun photometer network in Switzerland. *J. Geophys. Res.,* **106,** 27 537–27 554.

International Organization for Standardization, 1995: *Guide to the Expression of Uncertainty in Measurement.* ISO, 101 pp.

Jacovides, P. C., M. D. Steven, and D. N. Asimakopoulos, 2000: Spectral solar irradiance and some optical properties for various polluted atmospheres. *Sol. Energy,* **69,** 215–227.

Kasten, F., and A. T. Young, 1989: Revised optical airmass tables and approximation formula. *Appl. Opt.,* **28,** 4735–4738.

Kaufman, Y. J., A. Gitelson, A. Karnieli, E. Ganor, R. S. Fraser, T. Nakajima, S. Mattoo, and B. N. Holben, 1994: Size distribution and scattering phase function of aerosol particles retrieved from sky brightness measurements. *J. Geophys. Res.,* **99,** 10 341–10 356.

Kiedron, P. W., J. J. Michalsky, J. L. Berndt, and L. C. Harrison, 1999: Comparison of spectral irradiance standards used to calibrate shortwave radiometers and spectroradiometers. *Appl. Opt.,* **38,** 2432–2439.

Martinez-Lozano, J. A., M. P. Utrillas, F. Tena, and V. E. Cachorro, 1998: The parameterisation of the atmospheric aerosol optical depth using the Ångstrom power law. *Sol. Energy,* **63,** 303–311.

Michalsky, J. J., 1988: The Astronomical Almanac's algorithm for approximate solar position (1950–2050). *Sol. Energy,* **40,** 227–235.

——, J. A. Schlemmer, W. E. Berkheiser, J. L. Berndt, L. C. Harrison, N. S. Laulainen, N. R. Larson, and J. C. Barnard, 2001: Multiyear measurements of aerosol optical depth in the Atmospheric Radiation Measurement and Quantitative Links Programs. *J. Geophys. Res.,* **106,** 12 099–12 107.

Molineaux, B., P. Ineichen, and N. O'Neill, 1998: Equivalence of pyrheliometric and monochromatic aerosol optical depths at a single key wavelength. *Appl. Opt.,* **37,** 7008–7018.

Myers, D. R., 1989: Estimates of uncertainty for measured spectra in the SERI spectral solar radiation data base. *Sol. Energy,* **43,** 347–353.

Riordan, C., D. Myers, M. Rymes, R. Hulstrom, W. Marion, C. Jennings, and C. Whitaker, 1989: Spectral solar radiation database at SERI. *Sol. Energy,* **42,** 67–79.

Robinson, N., Ed.,1966: *Solar Radiation.* Elsevier, 347 pp.

Russell, P. B., and Coauthors, 1993: Pinatubo and pre-Pinatubo optical-depth spectra: Mauna Loa measurements, comparisons, inferred particle size distributions, radiative effects and relationship to lidar data. *J. Geophys. Res.,* **98,** 22 969–22 985.

Schmid, B., and C. Wehrli, 1995: Comparison of sun photometer calibration by use of the Langley technique and the standard lamp. *Appl. Opt.,* **34,** 4500–4512.

——, P. R. Spyak, S. F. Biggar, C. Wehrli, J. Sekler, T. Ingold, C. Mätzler, and N. Kämpfer, 1998: Evaluation of the applicability of solar and lamp radiometric calibrations of a precision sun photometer operating between 300 and 1025 nm. *Appl. Opt.,* **37,** 3923–3941.

Van Roozendael, M., and Coauthors, 1997: Ground-based observations of stratospheric NO_2 at high and midlatitudes in Europe after the Mount Pinatubo eruption. *J. Geophys. Res.,* **102,** 19 171–19 176.

Wilson, S. R., and B. W. Forgan, 2002: Aerosol optical depth at Cape Grim, Tasmania, 1986–1999. *J. Geophys. Res.,* **107,** 4068, doi: 10.1029/2001JD000398.

Young, A. T., 1980: Revised depolarization corrections for atmospheric extinction. *Appl. Opt.,* **19,** 3427–3428.